Development 129, 2317-2327 (2002)
Printed in Great Britain © The Company of Biologists Limited
DEV1759

A role for *iro1* and *iro7* in the establishment of an anteroposterior compartment of the ectoderm adjacent to the midbrain-hindbrain boundary

Motoyuki Itoh, Tetsuhiro Kudoh, Michael Dedekian, Cheol-Hee Kim and Ajay B. Chitnis*

Laboratory of Molecular Genetics, NICHD/NIH, Bethesda, MD 20892, USA
*Author for correspondence (e-mail: chitnisa@mail.nih.gov)

Accepted 19 February 2002

SUMMARY

We have identified a novel Iroquois (Iro) gene, *iro7*, in zebrafish. *iro7* is expressed during gastrulation along with *iro1* in a compartment of the dorsal ectoderm that includes the prospective midbrain-hindbrain domain, the adjacent neural crest and the trigeminal placodes in the epidermis. The *iro1* and *iro7* expression domain is expanded in *headless* and *masterblind* mutants, which are characterized by exaggerated Wnt signaling. Early expansion of *iro1* and *iro7* expression in these mutants correlates with expansion of the midbrain-hindbrain boundary (MHB) domain, the neural crest and trigeminal neurons, raising the possibility that *iro1* and *iro7* have a role in determination of these ectodermal derivatives. A knockdown of *iro7* function revealed that *iro7* is essential for the determination of neurons in the trigeminal placode. In addition, a knockdown of both *iro1* and *iro7* genes uncovered their essential roles in neural crest development and establishment of the isthmic organizer at the MHB. These results suggest a new role for Iro genes in establishment of an ectodermal compartment after Wnt signaling in vertebrate development. Furthermore, analysis of activator or repressor forms of *iro7* suggests that *iro1* and *iro7* are likely to function as repressors in establishment of the isthmic organizer and neural crest, and Iro genes may have dual functions as repressors and activators in neurogenesis.

Key words: Midbrain-hindbrain boundary, Trigeminal ganglia, Neural crest, Patterning, Compartment, Morpholino, Zebrafish

INTRODUCTION

The Iroquois (Iro) genes were discovered in *Drosophila* for their role in formation of sensory bristles in the dorsal mesothorax or notum of the fly (Dambly-Chaudiere and Leyns, 1992; Leyns et al., 1996). Further studies showed that the Iro locus encodes factors essential for the expression of proneural genes in the *achaete-scute* complex that are necessary for determination of sensory organ precursors (Gomez-Skarmeta et al., 1996). *Drosophila* has three Iro genes, *araucan* (*ara*), *caupolican* (*caup*) and *mirror* (*mirr*), and together they form the Iroquois complex (Iro-C). Molecular characterization of the Iro genes in *Drosophila* has allowed the identification of homologs in *C. elegans* and several vertebrates, including *Xenopus*, mouse, zebrafish, chick and human (Bao et al., 1999; Bellefroid et al., 1998; Bosse et al., 2000; Bosse et al., 1997; Christoffels et al., 2000; Cohen et al., 2000; Funayama et al., 1999; Gomez-Skarmeta et al., 1998; Goriely et al., 1999; Kudoh and Dawid, 2001; Ogura et al., 2001; Peters et al., 2000; Tan et al., 1999; Wang et al., 2001). The Iro genes encode proteins that show a strong similarity in their homeodomain and all contain a characteristic motif named the Iro box. Based on these features, the Iro products constitute a unique class of proteins within the TALE super-class of atypical homeodomain proteins (Burglin, 1997).

Analysis of Iro function in many developmental contexts and different model systems has now defined a broader role for these genes during development. During early development, these genes appear to have a role in defining the identity of large territories. In *Drosophila* their early expression defines dorsal eye, head and mesothorax territories (Cavodeassi et al., 1999; Cavodeassi et al., 2000; Diez del Corral et al., 1999). Later, the Iro genes have a role in the subdivision of such large territories into subdomains. For example, while they have an early role in defining the entire notum, later the Iro genes are required to specify the identity of the lateral notum where they are essential for expression of proneural genes and sensory bristle formation (Diez del Corral et al., 1999).

Analysis of Iro function in *Xenopus* has shown that these genes have similar roles in vertebrate development. The early expression of *Xiro1* and *Xiro2* in the dorsal ectoderm at the beginning of gastrulation and the effects of ectopic expression of *Xiro1* are consistent with an early role in establishment of neural fate in a large territory of the dorsal ectoderm (Gomez-Skarmeta et al., 2001). At a later stage, expression of *Xiro1* and *Xiro2* becomes restricted to two stripes within the neural plate that extend caudally from midbrain-hindbrain boundary (MHB). Expression of *Xiro1* and *Xiro2* in this restricted domain along with *Xiro3* suggests a late role in determining the expression of the proneural gene *Xenopus achaete-scute homolog 3* (*XASH3*) in a specific subdomain of the neural tube where neuronal precursors may be generated (Bellefroid et al., 1998; Gomez-Skarmeta et al., 1998). These studies suggest that vertebrate Iro genes function to establish cell fate in the

neural plate in a manner that is similar to *Drosophila*. However, loss-of-function studies have not defined how Iro genes contribute to development of specific territories in the neurectoderm during development.

In this study, we have examined roles of two zebrafish Iro genes: *iro1* and a novel Iro family member, *iro7*. We focus on two related issues, the role of these genes in neurogenesis and their role in determining the development of a large territory in the neurectoderm. We characterized their ability to induce expression of the proneural gene, *neurogenin1* (*ngn1*) and examined how a knockdown of these genes affects the development of tissues within an anteroposterior compartment defined by their early expression. Finally, by exploiting repressor or activator fusions, we determine how these homeodomain proteins affect transcription of target genes.

MATERIALS AND METHODS

Zebrafish maintenance and mutants

Zebrafish were raised and maintained under standard conditions. To collect maternal zygotic *headless*^{m881} mutant embryos, heterozygous males and homozygous females were crossed (Kim et al., 2000). In this study, we also used *no isthmus* (*noi*^{tu29a}) and *acerebellar* (*ace*^{ti282a}) mutants (Brand et al., 1996; Lun and Brand, 1998; Reifers et al., 1998).

Identification of *iro1* and *iro7*

iro1 was cloned during a random in situ based screen. *iro7* was initially identified as an EST (fc24a10) as an unknown Iro family gene. To obtain the 5′ region of *iro7*, 5′ RACE was performed using a tailbud cDNA library made by the SMART RACE cDNA amplification kit (Clontech). Sequences were deposited in GenBank under Accession Numbers AF414133 (*iro7*) and AF414134 (*iro1*). Sequence alignment was analyzed by J. Hein's method with PAM250 residue weight table using DNASTAR software. *iro7* was mapped on the LN54 radiation hybrid panel (Hukriede et al., 1999) using the primers 5′-AAATCTGACGAGGAGGATGAGGAAGAAGAG-3′ and 5′-TTCATTGACTTTGTTTGAGAAGGTCGTGTG-3′.

Whole mount in situ hybridization, antibody or β-galactosidase staining

For *iro1*, full-length cDNA was used as a template for making RNA probe (*Xho*I/T7). For *iro7*, the 3′ region of a cDNA containing approximately 750 bp was used for making RNA probe (*Sal*I/SP6). Zebrafish *gbx1* was found by EST search (fj77a06) and the coding fragment was subcloned into pCRIITOPO for RNA probe synthesis (*Not*I/SP6). Other plasmids that have been used to make in situ probes have been published previously: *otx2* (Li et al., 1994; Mori et al., 1994), *pax2.1* (*pax2a* – Zebrafish Information Network) (Krauss et al., 1991), *hoxb1b* (Alexandre et al., 1996), *ngn1* (*neurod3* – Zebrafish Information Network) (Blader et al., 1997; Kim et al., 1997), *fkd6* (*foxd3* – Zebrafish Information Network) (Odenthal and Nusslein-Volhard, 1998), *krox20* (*egr2* – Zebrafish Information Network) (Oxtoby and Jowett, 1993), *huC* (*elavl3* – Zebrafish Information Network) (Good, 1995; Kim et al., 1996) and *gata2* (Detrich et al., 1995). Double in situ using digoxigenin- and fluorescein-labeled RNA probes and antibody staining were performed as described (Itoh and Chitnis, 2001; Jowett, 2001). To detect β-galactosidase activity, embryos co-injected with various synthesized mRNA, were fixed in 4% paraformaldehyde overnight at 4°C and stained by either X-gal or salmon-β-D-galactoside (Biosynth).

Constructs

iro1 and *iro7* cDNA fragments encoding full-length protein were subcloned into the pCS2+ vector. To generate En-*iro7*HD and VP16-*iro7*HD, we amplified a fragment by PCR with primers 5′-CCGCTCGAGCCGTATCACCAAGCTCTCCTCGGA-3′ and 5′-GCTCTAGATTTTCCTTTGGACGCCCAGCT-3′. The amplified fragment was digested with *Xho*I and *Xba*I, and subcloned into pCS2-En or pCS2-VP16 (Kawahara et al., 2000). To make ΔN-*iro1* and ΔN-*iro7* constructs that lacked the morpholino antisense oligo (MO1 or MO7)-binding site, fragments were amplified by PCR using primers: 5′-CGGGATCCATGGAGGGAAGCTCGGACAACAGCGCA-3′ and 5′-GCTCTAGAAGAAATTGTCTTCAAAGCGCGTTGTG-3′ for the ΔN-*iro1* construct, 5′-CGGGATCCAACTTCTTCATGGACAGAA-ACATCAACATG-3′ and 5′-CGTCTAGAAGTTGACTTTGTTTGA-GAAGGTCGTGTGT-3′ for the ΔN-*iro7* construct, and they were subcloned in the *Bam*HI/*Xba*I sites of the pCS2+ vector.

mRNA and morpholino antisense oligo injection

For microinjection of mRNA, constructs were linearized and transcribed with SP6 RNA polymerase using the mMessage mMachine Kit (Ambion). For injection of wild type *iro1*, *iro7*, En-*iro7*HD and VP-*iro7*HD mRNA, we injected those mRNA into embryos at the16-64 cells stage to prevent gastrulation defects.

Morpholinos (Gene Tools) were resuspended in DEPC water and stored at –20°C. The sequences of the morpholinos used were 5′-GCGTGGAGAGGACGGCATTACACCC-3′ for *iro1* and 5′-GCAAACCCCGTTGATGAAGCAGGCA-3′ for *iro7*. The oligos were injected into one- to two-cell stage embryos.

In vitro translation

Iro1 and Iro7 protein were synthesized in the presence or absence of morpholino for *iro1* or *iro7* using TNT coupled reticulocyte lysate systems (Promega). Proteins were made from CS2+ *iro1* and CS2+ *iro7* plasmid (0.5 μg each) and labeled with [^{35}S] methionine. After the translation reaction was complete, reaction mixtures were subject to SDS-PAGE. The dried gel was exposed to X-ray film.

RESULTS

Cloning of zebrafish *iro1* and *iro7*

We identified two zebrafish Iro genes, *iro1* and *iro7* in a zebrafish EST database and in an in situ-based screen for genes with interesting expression patterns (Kudoh et al., 2001). A full-length 1.9 kb cDNA encoding 419 amino acids of *iro1* was obtained from the plasmid library used for the in situ-based screen. 5′ RACE was performed with a tailbud stage library to obtain the full coding sequence for *iro7*. This yielded a 1.3 kb cDNA encoding 314 amino acids of *iro7*.

The two uncharacterized Iro genes were identified as *iro1* and *iro7* based on a comparison of their sequences with previously identified members of the Iro family. Comparison of *iro1* with other members of family indicates that *iro1* is the *Irx1* ortholog with overall amino acid similarity of 47.6% and 44.0%, to *Xiro1* and mouse *Irx1*, respectively. Zebrafish *iro1* was independently characterized by another group that came to the same conclusion (Wang et al., 2001). However, *iro7* has a sequence that is very divergent from the six previously described Irx orthologs and so has been designated as *iro7*. It has also recently been independently characterized by Lecaudy et al. (Lecaudy et al., 2001).

iro7 may be a novel paralogue of *iro1* and *iro3* in zebrafish

Analysis of the human and mouse genome has suggested that there are a total of six Iroquois (Irx) family members in

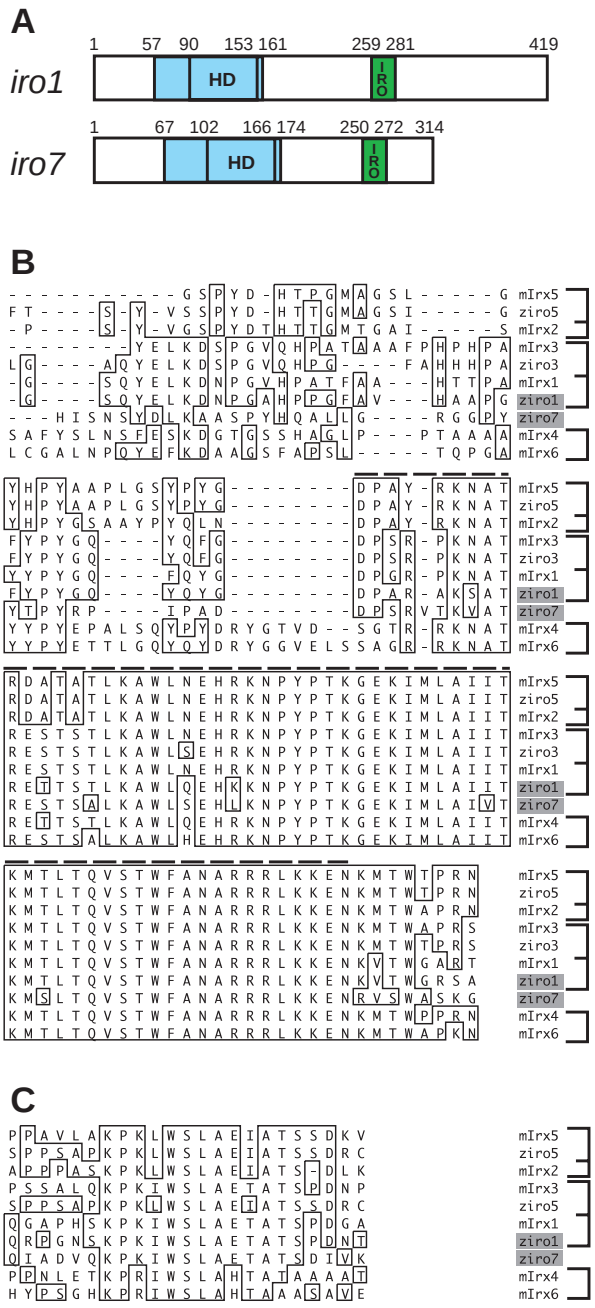

Fig. 1. Sequence alignment of zebrafish and mouse Iroquois proteins. (A) Schematic structure of Iro1 and Iro7. HD, homeodomain; IRO, Iro box. (B) Alignment of zebrafish Iro1, Iro3, Iro5 and Iro7 (ziro1, 3, 5 and 7), and mouse Irx1-Irx6 (mIrx1-Irx6) in part of the N-terminal domain and the homeodomain (blue shaded box in A); broken line represents the homeodomain. (C) Alignment of zebrafish and mouse Iro genes in the IRO box domain (green shaded box in A). Brackets in the right margin show orthologs and paralogs with most similarity (B,C). (D) Percentage similarity of amino acids between mouse Irx (MUS IRX1-IRX6) and zebrafish Iro (ZEF Iro1, Iro3, Iro5 and Iro7) proteins in the region shown in B. Each mouse Irx from the IrxA cluster is shown together with its paralog from the IrxB cluster.

mammals (Ogura et al., 2001; Peters et al., 2000). The six murine genes are in two tightly linked complexes with three genes in each cluster: *Irx1*, *Irx2* and *Irx4* are on chromosome 13 and form the IrxA cluster, while their respective paralogues *Irx3*, *Irx5* and *Irx6*, are on chromosome 8 and form the IrxB cluster (Peters et al., 2000).

Phylogenetic analysis of the six murine Irx genes was facilitated by comparing their amino acid sequence in two relatively conserved domains, the N-terminal and homeodomain region [Fig. 1A (shown in blue), Fig. 1B] and the Iro box domain [Fig. 1A (shown in green), Fig. 1C]. We compared these two regions in the six murine Irx genes with corresponding domains of zebrafish *iro1*, *iro3*, *iro5* and *iro7* (Fig. 1B,C). We found that zebrafish *iro1*, *iro3* and *iro5* have most similarity (Fig. 1D, shown in red) with their mouse orthologs *Irx1*, *Irx3* and *Irx5*, while the next best similarity (Fig. 1D, shown in blue) is with mouse paralogs *Irx3*, *Irx1* and *Irx2*, respectively. However, *iro7* is less similar to other members except in the homeodomain (Fig. 1B, broken line) and Iro box (Fig. 1C).

In zebrafish, map locations of *iro1*, *iro3* and *iro5* are consistent with the genomic organization described in mouse. Zebrafish *iro1* maps to Linkage Group (LG) 19, while zebrafish *iro3* and *iro5* map together on LG7, suggesting that, like *Irx3* and *Irx5* in mouse, the later are members of one cluster (Wang et al., 2001). Interestingly, *iro7* does not map to either LG19 or to LG7, but to LG23, close to Z5526 on the LN54 radiation hybrid panel where it is not clear if *iro7* is a part of an additional Iro gene cluster or whether it reflects a break up of an extant cluster that might have occurred during teleost evolution.

Expression patterns of *iro1* and *iro7*

Expression of *iro1* and *iro7* begins around the dome stage. Whole-mount in situ hybridization shows that *iro1* is almost undetectable at the dome stage, while in some embryos *iro7* is widely expressed at low levels (Fig. 2A,J). By the shield stage, their expression becomes more clearly defined and both genes are expressed in a similar pattern in two distinct domains of the embryo. They are expressed in the dorsal epiblast where their expression includes the prospective neurectoderm (Lecaudey et al., 2001; Wang et al., 2001) and adjacent to the lateral margin in the hypoblast where their expression is excluded from the shield (Fig. 2B,K).

At 75% epiboly, although expression of *iro1* and *iro7* is transiently retained at the anterior edge of the neurectoderm (data not shown), it is lost from much of the rostral neurectoderm and it becomes prominent in the prospective midbrain-hindbrain region (Fig. 2C,L). The limits of this expression domain were defined by comparison with genes expressed in various compartments of the forebrain, midbrain

D

	MUS IRX1 A	MUS IRX3 B	MUS IRX2 A	MUS IRX5 B	MUS IRX4 A	MUS IRX6 B
ZEF iro1	83.0	77.5	65.7	68.4	68.0	64.4
ZEF iro3	81.9	94.1	70.6	74.7	69.9	70.3
ZEF iro5	69.0	72.3	89.3	97.0	67.9	67.3
ZEF iro7	67.0	64.0	59.4	62.4	58.7	61.7

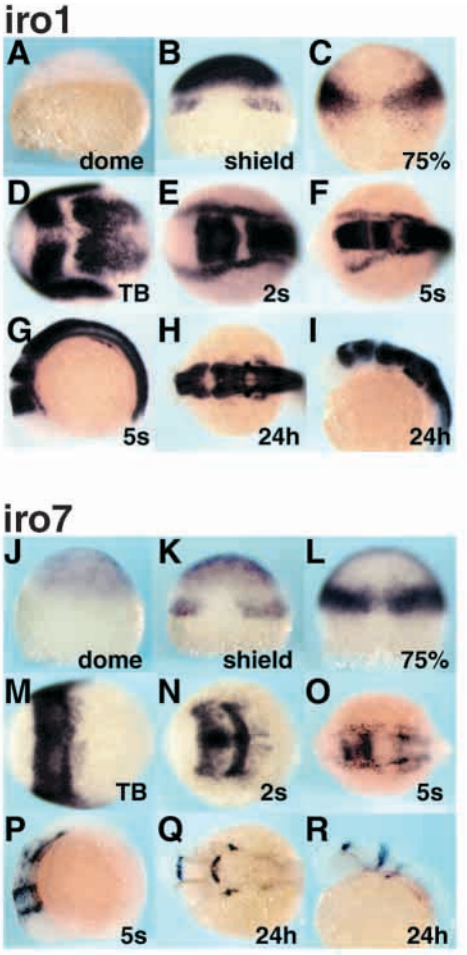

Fig. 2. Expression patterns of *iro1* and *iro7* at early embryonic stages. (A-I) *iro1* expression. (J-R) *iro7* expression. (A-C,J-L) Dorsal view of *iro1* and *iro7* expression at blastula and gastrula stages. Anterior is towards the top. *iro1* and *iro7* show similar patterns of expression until the late gastrula stage. (D-G,M-P) Dorsal view of *iro1* and *iro7* expression at the tailbud stage (TB) and early segmental stages (2s, 2 somites; 5s, 5 somites), anterior towards the left. (G,P) Viewed from side. Expression of *iro1* and *iro7* begins to diverge by the end of the gastrula stage. At 24 hours post fertilization (24h) (H,I,Q,R), expression of *iro1* is broad, while *iro7* expression is much more restricted (H,Q, dorsal view; I,R, side view).

and hindbrain at 80% epiboly. At this stage the domain of *iro1* and *iro7* expression overlaps at its rostral edge with the most caudal expression of *otx2*, a marker of prospective forebrain and midbrain. *pax2.1*, a marker of the prospective midbrain-hindbrain boundary (MHB) is expressed within the expression domains of both Iro genes (Fig. 3A,B,E,F) and their expression overlaps with *gbx1* in the prospective hindbrain beginning at rhombomere 1 (Fig. 3C,G). The caudal limit of the *iro1* and *iro7* expression is defined by *hoxb1b*, whose expression identifies neurectoderm caudal to rhombomere 4 (McClintock et al., 2001). Its expression abuts *iro1* and overlaps slightly with *iro7*, whose expression extends slightly more caudally than *iro1* at this stage (Fig. 3D,H). These comparisons show that by 80% epiboly, expression of *iro1* and *iro7* defines a compartment of the neurectoderm that extends from the midbrain to rhombomere 4 in the hindbrain.

By tailbud stage, differences in expression of the two genes become more apparent. While both *iro1* and *iro7* continue to be expressed in the prospective midbrain-hindbrain region, *iro1* expression expands at its lateral margins caudally into domains where peripheral ganglia will develop; in addition, its expression begins in the caudal neurectoderm (Fig. 2D,M). By early somitogenesis, a gap in expression at the midbrain-hindbrain boundary (MHB) splits midbrain-hindbrain expression of *iro1* and *iro7* into two subdomains (Fig. 2E-G,N-P). Both genes are expressed in a subdomain rostral to *pax2.1* in the midbrain. Expression of *iro1* just caudal to *pax2.1* identifies a caudal subdomain in rhombomere 1 (Fig. 3K,O). Comparison with *krox20*, which is expressed in rhombomeres 3 and 5, reveals a caudal subdomain of *iro7* expression in rhombomeres 3 and 4 (Fig. 3P), and expression of *iro1* in the caudal neurectoderm beginning at rhombomere 5 (Fig. 3L). As somitogenesis continues, expression of *iro1* remains over a broad area as its expression extends into the developing caudal neural tube, while *iro7* becomes progressively restricted (Fig. 2F-I,O-R).

Consistent with a role for Iro genes in controlling the expression of vertebrate proneural genes, *iro1* and *iro7* are expressed in partially overlapping patterns that cover many domains of *ngn1* expression in the neurectoderm at the tailbud stage (Fig. 3I,M). *iro1* and *iro7* expression extends laterally outside the neurectoderm to include domains of *ngn1* expression in developing trigeminal placodes (Fig. 3I,M, arrowhead). Just medial to this domain, expression of *iro1* and *iro7* overlaps with expression of *fkd6*, a marker of premigratory neural crest cells (Odenthal and Nusslein-Volhard, 1998) (Fig. 3J,N). In the caudal neurectoderm, expression of *iro1*, but not *iro7*, overlaps with *ngn1*, where this proneural gene defines longitudinal proneuronal domains where early neurons differentiate (Fig. 3I).

The size of the *iro1* and *iro7* expression domain is expanded by exaggerated Wnt signaling

iro1 and *iro7* are expressed in a caudal compartment of the anterior neurectoderm that includes the prospective MHB domain, the adjacent neural crest and trigeminal neurons. In maternal zygotic (MZ) *hdl* mutants, failure to repress Wnt target genes adequately in the anterior neurectoderm leads to exaggerated Wnt signaling and a rostral expansion of the trigeminal neurons, the MHB domain and cranial neural crest, identified by expression of *ngn1*, *pax2.1* and *fkd6*, respectively (Kim et al., 2000) (Fig. 4C,D). Examination of MZ *hdl* mutants reveals expansion of the *iro1* and *iro7* expression domain (Fig. 4A, B), which becomes evident by 75% epiboly (data not shown). It is likely that this expansion predominantly reflects a shift in the rostral boundary of *iro1* and *iro7* expression, as the expression of hindbrain markers *krox20* (Fig. 4D) and *gbx1* (data not shown) is not appreciably altered in *hdl* mutants. A similar expansion of *iro1* and *iro7* expression was observed in *masterblind* (*mbl*) mutants (data not shown) that are also characterized by exaggerated Wnt signaling, in this case due to a mutation in *axin*, which normally promotes degradation of β-catenin, an effector of Wnt signaling (Heisenberg et al., 2001). These observations suggest that the size of the *iro1* and *iro7* expression domain is determined by the level of Wnt signaling in the anterior neurectoderm.

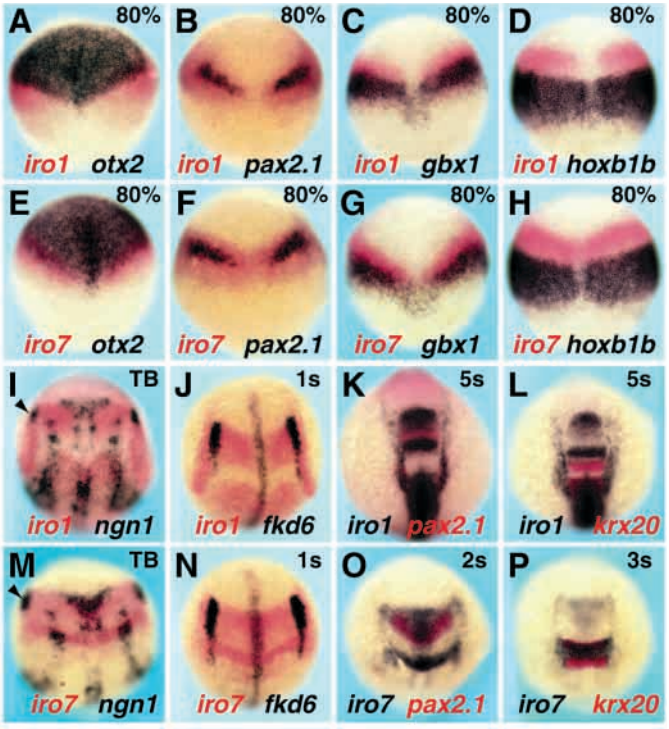

Fig. 3. Double in situ hybridization defining the domains of *iro1* and *iro7* expression. Expression patterns of *iro1* (A-D,I-L) and *iro7* (E-H,M-P). (A-H) Double in situ hybridization with *otx2* (A,E), with *pax2.1* (B,F), with *gbx1* (C,G), and with *hoxb1b* (D,H) at 80% epiboly. (I,M) At the tailbud stage, *iro1* and *iro7* are expressed in partially overlapping patterns with *ngn1*. (J,N) neural crest cells marked by *fkd6* expression are within a domain where *iro1* and *iro7* are expressed. (K,O) By early somitogenesis, expression of *iro1* and *iro7* is excluded from the MHB region marked by *pax2.1*. (L,P) *iro1* and *iro7* are expressed in different locations in the hindbrain: *iro1* is expressed in rhombomere 1 and caudally from rhombomere 5, while *iro7* is expressed in rhombomeres 3 and 4. (A-P) Anterior towards the top, dorsal view.

iro7 is essential for determination of trigeminal neurons

Embryos were injected with antisense morpholino oligos complementary to the N-terminal of *iro1* (MO1) and *iro7* (MO7) to examine the function of these Iro genes. To demonstrate that both MO1 and MO7 were effective at knocking-down translation of respective Iro transcripts, an in vitro translation assay was done to compare translation of *iro1* and *iro7* from plasmids (mixture of 0.5 μg each) in the presence of different amounts of the morpholinos. Gels comparing expression of ^{35}S-labeled Iro1 and Iro7 in the presence of increasing concentrations (from 12.5 ng to 12.5 μg) of either MO1 or MO7 showed that each morpholino specifically inhibits translation of the targeted Iro gene in a dose-dependent manner (Fig. 5J).

Examination of *ngn1* expression in injected embryos at the one-somite stage revealed that 10 ng MO1 has no effect on expression of *ngn1* but 10 ng MO7, directed against *iro7*, leads to a loss of *ngn1* expression in the developing trigeminal ganglia (95%, *n*=22) (Fig. 5A-D). MO7 also affected expression of *ngn1* in developing neurons within the neural plate, including those in rhombomeres 2 and 4; however, the effects on CNS neurons have not yet been fully examined. To show that effects of MO7 are specifically due to its ability to knockdown *iro7* function, MO7 was injected with mRNA encoding an engineered form of *iro7* (Δ*Niro7*) in which nine N-terminal amino acids were deleted to prevent hybridization with MO7. Embryos were first injected with MO7 at the one-cell stage so that both sides received the morpholino, and then in addition, one side was injected at the two-cell stage with Δ*Niro7* and β-galactosidase mRNA (to detect distribution of Δ*Niro7*transcripts). Embryos injected in such a manner revealed that co-expression of Δ*Niro7* with MO7 led to a recovery of *ngn1* expression in the trigeminal placode (Fig. 5D). To show that reduced *ngn1* expression in MO7-injected embryos prevents formation of trigeminal ganglia, MO1- and MO7-injected embryos were examined at 24 hpf with an antibody to acetylated α-tubulin that identifies differentiating neurons. Only MO7-injected embryos showed a loss of neurons in the trigeminal ganglia (83%, *n*=12) confirming that *iro7* has an essential role in determination of these neurons (Fig. 5E-G).

iro7 can induce expression of *ngn1* as either an activator or repressor

As a morpholino directed against *iro7* reduced expression of *ngn1* in the trigeminal ganglia, we examined if ectopic expression of *iro1* and *iro7* promotes expression of this proneural gene. Initially it was difficult to interpret the effects of ectopic *iro1* and *iro7* expression because widespread expression of those mRNA caused severe gastrulation defects. This problem was overcome by injecting single cells relatively late in development to restrict the domain of ectopic expression. Embryos injected with 50 pg *iro1* or *iro7* mRNA at the 16-to 64-cell stage and assayed at the tailbud stage revealed that both Iro genes could induce expression of *ngn1* in the neurectoderm ectoderm (Fig. 5D, data not shown) and the ventral ectoderm where this proneural gene is normally not expressed (*iro1*: 95%, *n*=19; *iro7*: 100%, *n*=24) (Fig. 5L,M).

To determine if *iro1* and *iro7* induce *ngn1* expression by acting as activators or repressors, we made engineered forms of *iro7*, expected to exclusively repress or activate Iro target genes. Plasmids encoding chimeric transcription factors (En-*iro7*HD and VP-*iro7*HD) were made by combining domains encoding the repressor domain of Engrailed (En) or the activation domain of VP16 (VP) with a fragment of the *iro7* homeodomain (*iro7*-HD) (Fig. 5K) (Conlon et al., 1996; Kessler, 1997). Though the chimeric constructs contained the *iro7* homeodomain, it was expected that the fusion proteins would bind target sequences for other Iro family members because of over 86% similarity between Iro genes in the homeodomain.

The effects of En-*iro7*HD and VP-*iro7*HD on *ngn1* expression were surprising: both repressor and activator forms of *iro7* were capable of inducing ectopic *ngn1* expression and the pattern of ectopic *ngn1* induced was unique in each case. Like *iro1* and *iro7*, 50 pg of En-*iro7*HD mRNA effectively induced *ngn1* expression in the ventral ectoderm (96%, *n*=27) (Fig. 5N). However, in contrast to the widespread or patchy expression induced by *iro1* and *iro7*, respectively (Fig. 5L,M), *ngn1* expression induced by En-*iro7*HD in the ventral ectoderm was typically in a discrete salt-and-pepper pattern (Fig. 5N). Injection of 50 pg of VP-*iro7*HD mRNA had very different

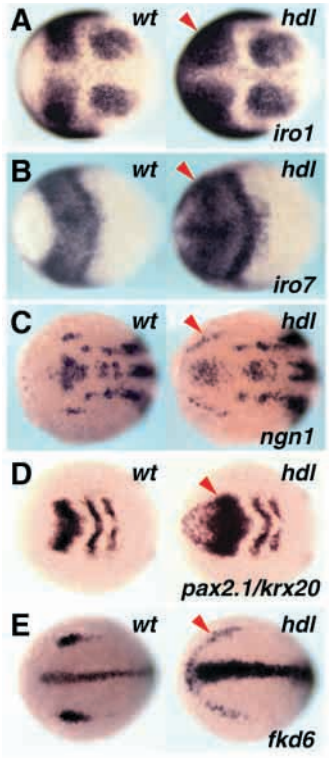

Fig. 4. Rostral expansion of trigeminal ganglia, the MHB domain, and the premigratory neural crest cells correlates with expansion of *iro1* and *iro7* in *headless* (*hdl*) mutants. (A,B) Expression of *iro1* (A) and *iro7* (B) is expanded rostrally in *hdl* mutants at the tailbud stage. (C-E) The trigeminal ganglia (C), MHB domain (D) and neural crest (E), marked respectively by *ngn1* expression at the one-somite stage (C), *pax2.1* at the three-somite stage (D) and *fkd6* at the tailbud stage (E), are expanded rostrally in *hdl* mutants. Expression of *krox20* (*krx20*) in the hindbrain is unaffected in *hdl* (D). Red arrowheads indicate anterior limit of expression of each gene in wild-type embryos for comparison.

effects. It was ineffective at inducing ectopic *ngn1* in the ventral ectoderm but was able to induce widespread ectopic *ngn1* expression within the neurectoderm (100%, *n*=24) (Fig. 5O). These data suggest that both activator and repressor forms of *iro7* can induce ectopic *ngn1* but they may achieve this by slightly different mechanisms in the ventral and dorsal ectoderm.

Previous studies have shown that *Xiro1* can function as a repressor to inhibit BMP expression and neuralize the ectoderm (Gomez-Skarmeta et al., 2001). One possibility is that *iro1*, *iro7* and the repressor En-*iro7*HD induce *ngn1* expression in the ventral ectoderm by inhibiting BMP signaling and neuralizing the ectoderm. Consistent with this possibility *iro1*, *iro7* and *En-iro7HD* can inhibit expression of a BMP target gene, *gata2* in the ventral ectoderm (*iro1*: 85%, *n*=39; *iro7*: 93%, *n*=30; En-*iro7*HD: 77%, *n*=30) (Fig. 5 P-S).

iro1 and *iro7* are necessary but not sufficient for determination of neural crest fate

The expression of *iro1* and *iro7* in a compartment that defines where trigeminal neurons, the neural crest and the MHB domain are located raised the possibility that these Iro genes not only have a role in determination of trigeminal neurons but they also regulate development of adjacent tissues in this compartment. To test this hypothesis, we examined the effects of *iro1* and *iro7* morpholinos on development of the cranial neural crest and the MHB domain.

Embryos injected with 10 ng MO1 showed a small decrease in *fkd6* expression, while injection of 10 ng MO7 resulted in little change; however, when 5 ng of MO1 and MO7 each were simultaneously injected, there was a clear reduction of *fkd6* expression in the neural crest (88%, *n*=25) (Fig. 6B-D). The specificity of this effect was revealed by the observation that the morpholinos never affected axial expression of *fkd6* (Fig. 6D). In addition, the reduction in *fkd6* expression induced by MO1 and MO7 was suppressed by co-injection of modified *iro1* and *iro7* transcripts (ΔN*iro1/7*) that lacked the N terminal sequences that the morpholinos were targeted against (Fig. 6E, arrowhead). These observations suggest that the overlapping expression of *iro1* and *iro7* determines the fate of *fkd6*-expressing neural crest cells in a partially redundant manner. Embryos injected with 50 pg of wild-type *iro1* or *iro7* mRNA, however, did not show much ectopic *fkd6* expression suggesting that while expression of *iro1* and *iro7* is necessary for *fkd6* expression, it is not sufficient to induce its expression (Fig. 6H,I). Activator and repressor forms of *iro7* revealed that they have opposite effects on neural crest formation: 50 pg of En-*iro7*HD mRNA induced a small increase in *fkd6* expression (Fig. 6J, arrowhead), while 50 pg of VP-*iro7*HD mRNA reduced expression of this neural crest marker (82%, *n*=33) (Fig. 6K). These observations suggest *iro1* and *iro7* act as repressors to determine formation of the cranial neural crest.

iro1 and *iro7* are essential for formation of the Midbrain-Hindbrain boundary and establishment of the isthmic organizer

To examine the role of *iro1* and *iro7* in establishment of the MHB domain and function of the isthmic organizer, we examined the effects of morpholinos, MO1 and MO7, on expression of genes that identify this domain at 24 hpf. Injection of 10 ng of MO1 or MO7 alone had subtle effects on expression of *eng2*, *pax2.1*, *fgf8* and *wnt1*, while injection of 5 ng each of MO1 and MO7 resulted in significant reduction or absence of their expression at the MHB domain (*eng2*: 69%, *n*=13; *pax2.1*: 87%, *n*=15; *fgf8*: 82%, *n*=11; *wnt1*: 92%, *n*=12) (Fig. 7A-D). Injection of MO1 alone also resulted in some decrease in *eng2* expression (Fig. 7A). Co-injection of MO1 and MO7 not only resulted in a loss of *pax2.1*, *fgf8* and *wnt1* expression in the MHB domain it also altered their expression in the forebrain and hindbrain. The morpholinos expanded *fgf8* expression in the forebrain and made *pax2.1* expression in the forebrain and otic vesicles more prominent (Fig. 7B,C). In part, the effects on *pax2.1* expression in the forebrain and otic vesicles may be accounted for by the slight delay in development caused by the injection of morpholinos, as at a slightly earlier stage of development expression of *pax2.1* is normally prominent in these domains. MO1 and MO7 injection also disrupted segmental *wnt1* expression in rhombomeres (Fig. 7D).

To address how early *iro1* and *iro7* work together in MHB formation, we examined embryos at the tailbud stage. We found injection of MO1 and MO7 together leads to a specific reduction of *pax2.1* expression (67%, *n*=12) (Fig. 7E) without causing a change in *wnt1* and *fgf8* expression (data not shown). The reduction in *pax2.1* expression induced by MO1 and MO7 was suppressed by co-injection of ΔN*iro1/7* (Fig. 7G, arrowhead). However, injection of 50 pg *iro1* mRNA resulted in ectopic expression of both *pax2.1* and *fgf8* at the tailbud stage (*pax2.1*: 100%, *n*=14; *fgf8*: 95%, *n*=19), while it had little effect on *wnt1* expression at this stage (Fig. 7H). Ectopic expression of 50 pg *iro7* mRNA also induced *fgf8* expression (73%, *n*=26), however, it had no effect on expression of *pax2.1* and in some embryos it reduced expression of *wnt1* (Fig. 7I).

As with injection of *iro1* mRNA, injection of 50 pg of En-*iro7*HD mRNA initiates ectopic expression of *pax2.1* and *fgf8*,

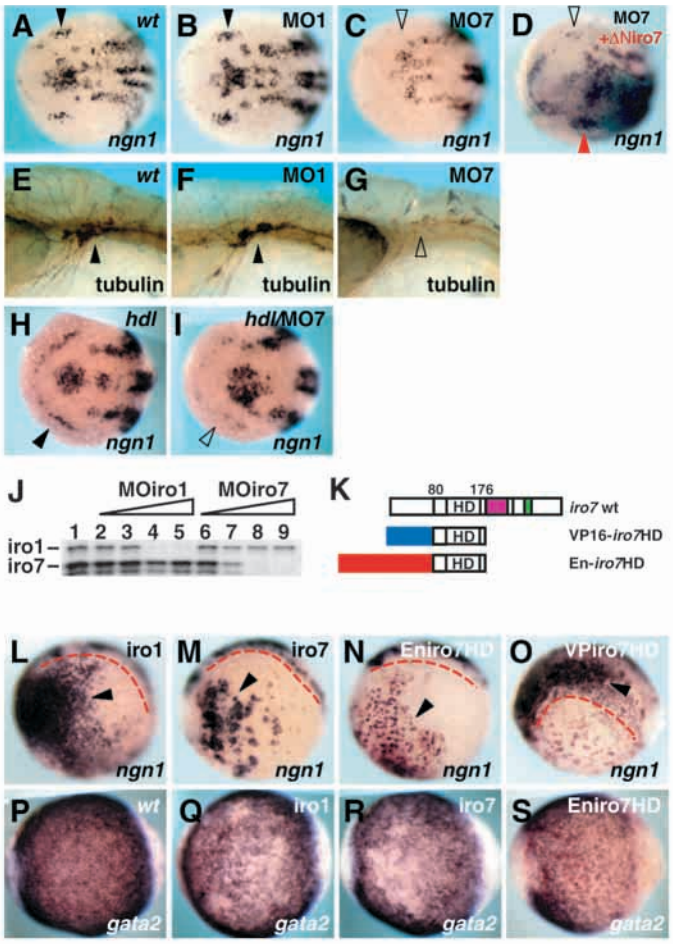

Fig. 5. The role of *iro1* and *iro7* in neurogenesis. (A-H) A knockdown of *iro1* and *iro7* with morpholino antisense oligos MO1 and MO7 reveals that *iro7* is essential for expression of the *ngn1* in trigeminal ganglia. Expression of *ngn1* in trigeminal ganglia (black arrowhead) is similar in uninjected (A) and MO1-injected embryos (B). Injection of MO7 leads to a loss of *ngn1* expression in the trigeminal ganglia (C, open arrowhead). The knockdown of *iro7* by MO7-injected at the one-cell stage is rescued on one side by co-injection with ΔN*iro7* mRNA (D). *ngn1* expression in the trigeminal is not lost (red arrowhead) on the side injected with ΔN*iro7* and *lacZ* mRNA, while it is reduced on the side MO7 was injected without *ΔNiro7* RNA (open arrowhead). The distribution of co-injected mRNA is visualized with a blue X-gal reaction product. (E-G) Examination of embryos at 24 hpf with an acetylated α-tubulin antibody reveals trigeminal neurons (black arrowhead) in uninjected and MO1-injected embryos but not in MO7-injected embryos (G, open arrowhead). (H,I) Expression of *ngn1* in trigeminal ganglia in *hdl* mutants (H, black arrowhead) is expanded to the anterior but its expression is lost in MO7-injected *hdl* mutants (I, open arrowhead). (J) Antisense morpholinos specifically block *iro1* and *iro7* translation. Radiolabeled proteins, Iro1 and Iro7, were synthesized simultaneously in vitro in the presence of an increasing log molar ratio (10^1-10^4) of morpholinos, *iro1* (MO1) or *iro7* (MO7), and were run out on a SDS-PAGE gel. Lane 1: control, no morpholino. Increasing amounts of MO1 (lane 2-5) and MO7 (lane 6-9) lead to a specific reduction in the synthesis of Iro1 and Iro7 protein, respectively. (K) Structure of two artificial constructs; top, wild-type *iro7*; middle, VP16-*iro7*HD, the homeodomain of *iro7* was fused to the activator region of VP16 herpes simplex virus (blue box); bottom, En-*iro7*HD, the homeodomain of *iro7* was fused to the *Drosophila* Engrailed repressor region (red box). Purple box represents acidic region; green represents the Iroquois box. (L-O) Ectopic expression of *iro1* and *iro7* mRNA induces relatively broad *ngn1* expression in the ventral ectoderm (arrowheads in L,M). En-*iro7*HD mRNA induces *ngn1* expression in a salt-and-pepper pattern in the ventral ectoderm (N), while VP16-*iro7*HD mRNA is more effective at inducing broad *ngn1* expression within the neural plate (O). (L-O) Anterior is towards the left, side view. Broken lines show the boundary between neural plate and ventral ectoderm. Embryos are at the three-somite stage. Distribution of ectopic mRNA is marked by red salmon-Gal staining to detect co-injected nuclear β-galactosidase activity. (P-S) Expression of *gata2* is reduced in *iro1* (Q), *iro7* (R), En-*iro7*HD (S) mRNA injected embryos when compared with uninjected control embryos (P). Embryos are at tailbud stage and viewed from ventral side.

but not *wnt1* (*pax2.1*: 94%, *n*=17; *fgf8*: 82%, *n*=17) (Fig. 7J). By contrast, injection of 50 pg VP-*iro7*HD mimics the combined effects of the two morpholinos. It prevents formation of the isthmus or the constriction between midbrain and hindbrain (Fig. 7L), and inhibits expression of *pax2.1*, *fgf8* and *wnt1*, genes that mark the isthmic organizer at 24 hpf (*pax2.1*: 100%, *n*=28; *fgf8*: 89%, *n*=19; *wnt1*: 83%, *n*=6) (Fig. 7K,M and data not shown). These data suggest that *iro1* and *iro7* are likely to function as repressors in initiating establishment of the MHB domain and the isthmic organizer.

Expansion of the MHB domain and adjacent tissues in *hdl* mutants is dependent on the function of *iro1* and *iro7*

Expansion of the MHB domain and the adjacent trigeminal ganglia and neural crest correlates with early expansion of *iro1* and *iro7* in *hdl* and *mbl* mutants, and establishment of these tissues appears normally dependent on *iro1* and *iro7* function (Fig. 4A-E). These observations suggest that expansion of the MHB domain and adjacent tissues is due to the early expansion of *iro1* and *iro7* gene expression in mutants with exaggerated Wnt signaling. To test this hypothesis, we examined expression of *pax2.1* and *fkd6* in MZ *hdl* mutants injected with MO1 and MO7, and *ngn1* in mutants injected with MO7 alone. The anterior expanded expression of *pax2.1* (100%, *n*=19), *fkd6* (95%, *n*=21) and *ngn1* (100%, *n*=16) was inhibited in morpholino-injected embryos, supporting the hypothesis that expansion of the MHB domain and adjacent tissues is dependent on expanded expression of *iro1* and *iro7* in mutants with exaggerated Wnt signaling (Fig. 5H,I, Fig. 6F,G, Fig. 7F).

DISCUSSION

Iro genes and primary neurogenesis

We have identified two zebrafish Iro genes, *iro1* and a novel zebrafish Iro family member, *iro7*, that are expressed during gastrulation in a dorsal compartment of the ectoderm. This compartment includes the prospective MHB domain, the adjacent cranial neural crest and neurons of the trigeminal ganglia. Our initial motivation in this study was to examine the role of these Iro genes in neurogenesis and in formation of the trigeminal neurons. Ectopic expression of both *iro1* and *iro7* led to ectopic expression of *ngn1* and a knockdown of *iro7*

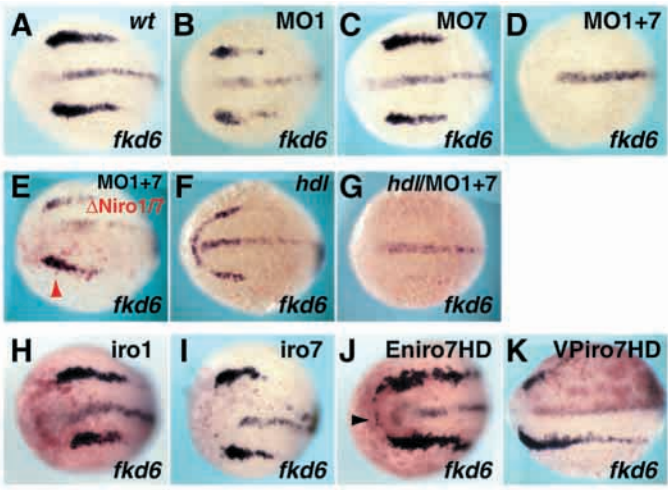

Fig. 6. *iro1* and *iro7* act together as repressors in neural crest formation. A combination of both morpholinos (MO1+7) causes a strong reduction of *fkd6* expression at an early somite stage (D) compared with either single morpholino MO1 (B), MO7 (C) or uninjected control embryos. (E) *fkd6* expression is recovered (red arrowhead) by ΔN*iro1* and ΔN*iro7* mRNA co-injection in MO1+MO7-injected embryos. (F, G) Expression of *fkd6* in *hdl* mutants (F) is expanded to the anterior but its expression is lost in MO1 and MO7 co-injected *hdl* mutants (G). Injection of *iro1* (H) and *iro7* (I) mRNA does not induce ectopic *fkd6* expression; however, En-*iro7*HD mRNA induces a little ectopic *fkd6* expression in the anterior neuroectoderm (J, arrowhead). By contrast, injection of VP16-*iro7*HD mRNA represses endogenous expression of *fkd6* (K). The distribution of injected mRNA is visualized with red salmon-Gal staining. All embryos are viewed from dorsal side and anterior is towards the left.

function led to a clear reduction in *ngn1* expression and differentiation of trigeminal ganglia. Together, these observations suggest that *iro7* has an essential role in determining the fate of trigeminal neurons and that its ectopic expression accounts in part for the expanded distribution of these neurons in *hdl* mutants. The knockdown of *iro7* also affected distribution of *ngn1* in the midbrain-hindbrain region; however, these effects have not been analyzed at this stage. The knockdown of *iro1* function had little effect on *ngn1* expression in the caudal neurectoderm (future spinal cord). This suggests that *iro1* function is redundant in this domain and that other unidentified Iro genes may be able to compensate for its loss.

iro1 and *iro7* are essential for development of an anteroposterior territory

An unexpected finding was the observation that a knockdown of *iro1* and *iro7* function not only affected *ngn1* expression in the trigeminal placode it also affected formation of adjacent neural crest cells and the MHB domain. Each of these tissues is a derivative of a different ectodermal compartment, epidermal, neural crest and neural, respectively, whose individual fates are determined by a number of signaling pathways that determine dorsoventral fate including BMP signaling (Chitnis, 1999; Marchant et al., 1998; Nguyen et al., 1998). All three domains, however, are contained within the anteroposterior compartment of the ectoderm where *iro1* and *iro7* are initially expressed. Together, these observations suggest that *iro1* and *iro7* are not just involved in regulating neurogenesis but are also essential for normal development of an anteroposterior compartment of the dorsal ectoderm. This conclusion is consistent with the emerging view that Iro genes, both in the fly and vertebrates are required at early stages of development to define large territories (Cavodeassi et al., 2001). However, this is the first loss-of-function study to define how Iro genes contribute to development of a large territory in the ectoderm during early vertebrate development.

Patterning of the neurectoderm by Wnt signaling mediated by Iro genes

Wnt signaling patterns the neurectoderm along the anteroposterior axis (Patapoutian and Reichardt, 2000). During early gastrulation, regulation of Wnt signaling plays an essential role in establishing forebrain, eye, midbrain and MHB territories in the anterior neuroectoderm (Bally-Cuif et al., 1995; Glinka et al., 1998; Heisenberg et al., 2001; Kim et al., 2000). Genes that determine the fate of the most rostral tissues in the anterior neurectoderm are dependent on mechanisms that repress Wnt signaling, while genes expressed in relatively caudal domains are dependent on relatively high levels of Wnt signaling. Ineffective repression of Wnt target genes in *hdl* mutants or reduced destruction of a Wnt effector in *mbl* mutants leads to exaggerated Wnt signaling in the anterior neurectoderm (Heisenberg et al., 2001; Kim et al., 2000). Increased Wnt signaling in *hdl* and *mbl* mutants is accompanied by a rostral expansion of *iro1* and *iro7* expression, suggesting that, as recently reported for *Xiro1* in *Xenopus* (Gomez-Skarmeta et al., 2001), Wnt signals regulate the size of the territory where these Iro genes are expressed. Loss-of-function studies in wild-type and *hdl* mutant backgrounds suggest that the territory of *iro1* and *iro7* expression not only defines the region within which trigeminal neurons, neural crest and the MHB domain are formed but the function of these Iro genes is essential for the development of these tissues. These observations suggest that Wnt signaling defines the identity of a caudal compartment of the anterior neurectoderm through the function of *iro1* and *iro7*.

iro1 and *iro7* are essential for establishment of the isthmic organizer

The isthmus is a specialized tissue with secondary organizer properties formed at the boundary between the midbrain and hindbrain. It eventually becomes the source of Wnt and FGF signals, and is essential for normal anteroposterior patterning of the adjacent midbrain and anterior hindbrain (Rhinn and Brand, 2001; Wurst and Bally-Cuif, 2001). Inhibition of *iro1* and *iro7* function with morpholinos leads to loss of the isthmus and patterning defects that suggest *iro1* and i*ro7* have an essential role in establishing a functional isthmic organizer.

Interactions between *pax2.1*, *wnt1* and *fgf8* play an early role in establishing and maintaining the isthmic organizer at the boundary of *gbx2* and *otx2* expression domains (Bally-Cuif et al., 1995; Lun and Brand, 1998; Reifers et al., 1998; Schwarz et al., 1997; Wurst and Bally-Cuif, 2001). While it is not yet clear how *iro1* and *iro7* regulate formation of the isthmic organizer, our data suggests that they have a relatively early role, as they are expressed in the midbrain-hindbrain domain before *otx2* and *gbx1*. They may also function by a mechanism that is independent of *otx2* and *gbx1*, because rostral expansion

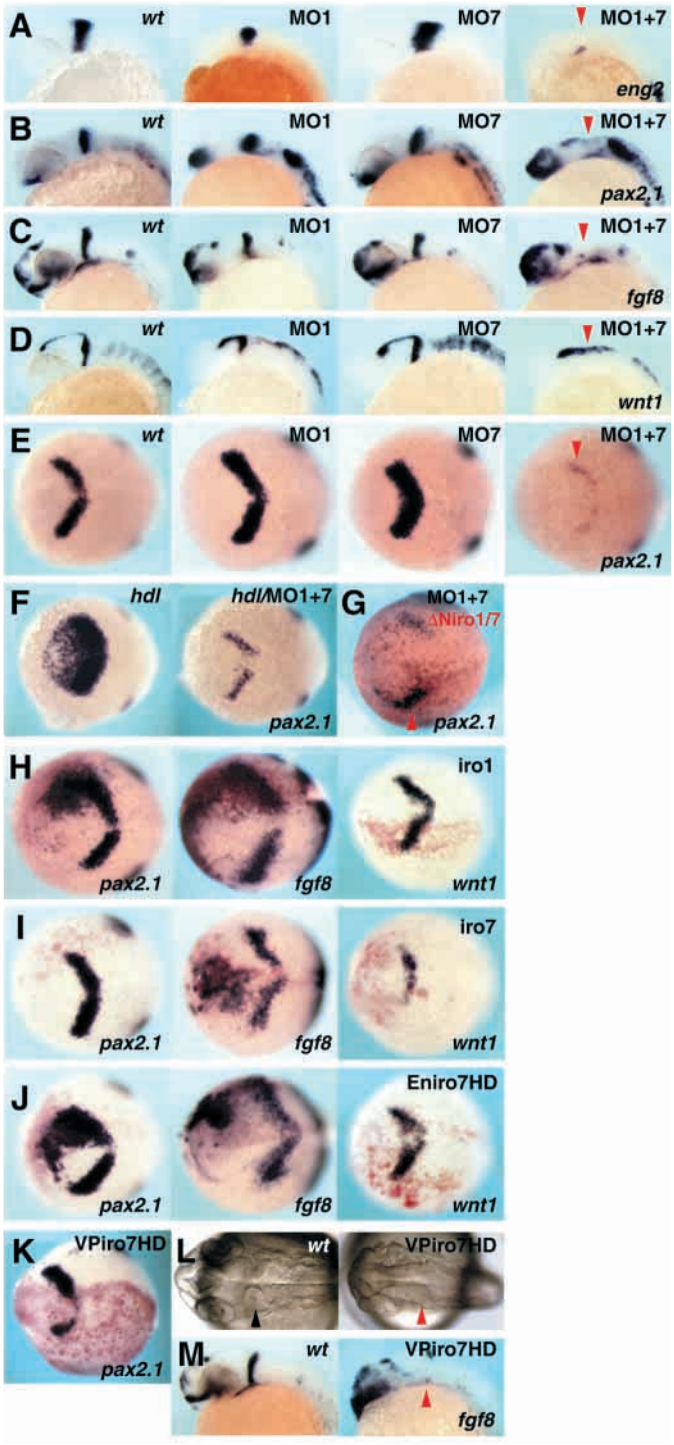

Fig. 7. *iro1* and *iro7* act together as repressors in formation of the MHB domain, while ectopic *iro1* or *iro7* induces the ectopic expression of MHB genes. (A-E) The effects of the *iro1* (MO1) and *iro7* (MO7) morpholinos on expression of MHB markers *eng2* (A), *pax2.1* (B), *fgf8* (C), *wnt1* (D) at 24 hpf and *pax2.1* (E) at tailbud stage. Red arrows show reduction of MHB markers. (F) Expression of *pax2.1* in *hdl* mutants (left) is expanded to the anterior but its expression is reduced in MO1 and MO7 co-injected *hdl* mutants (right). (G) Expression of *pax2.1* is recovered (red arrowhead) by ΔN*iro1* and ΔN*iro7* mRNA co-injection in double morpholino-injected embryos. (H-J) Embryos injected with *iro1* mRNA or En-*iro7*HD mRNA showed ectopic expression of *pax2.1* and *fgf8*, but not *wnt1* (F,H), while *iro7* mRNA induces *fgf8* and reduces *wnt1* (G). The distribution of injected mRNA is marked by red staining. (K-M) VP16-*iro7*HD mRNA injected embryos show loss of *pax2.1* expression (K) at tailbud stage and the isthmus at the MHB region (L, arrowhead) and loss of *fgf8* expression (M) at 24 hpf. Anterior is towards the left (A-M). Embryos are viewed from the left side (A-D,M) or dorsal (E-L).

of Iro genes in *hdl* mutants is not accompanied by any noticeable change in *otx2* and *gbx1* expression (data not shown).

In contrast, reduced *iro1* and *iro7* function results in loss of *pax2.1*, the earliest marker described so far for the MHB domain in zebrafish. Furthermore, while ectopic expression of *iro1* induces expression of *pax2.1* and *fgf8*, expression of *iro1* and *iro7* remains unaffected in mutants where the function of *pax2.1* (*noi*) and *fgf8* (*ace*) is lost (data not shown). Together, these observations suggest a relatively early role for Iro genes in initiation of *pax2.1* expression and establishment of the MHB domain. While *iro1* and *iro7* are required to initiate *pax2.1* expression, they are not required for the initial expression of *wnt1* or *fgf8*. This suggests that *wnt1* and *fgf8* expression in the MHB may be established independently by alternative pathways, as has been suggested by previous studies (Lun and Brand, 1998; Rhinn and Brand, 2001; Wurst and Bally-Cuif, 2001).

Does *iro7* act as a repressor or an activator?

Iroquois homeoproteins have been suggested to act as either activators or repressors in different experimental model systems and developmental contexts. In *Drosophila* neurogenesis, *ara* and *caup* can bind to the promoter of the *achaete-scute* proneural genes and function as activators (Gomez-Skarmeta et al., 1996). However, *Xiro1* functions as a repressor to inhibit BMP expression and neuralize the ectoderm (Gomez-Skarmeta et al., 2001). Our study suggests that in the context of neural crest and MHB formation, *iro1* and *iro7* are likely to function as repressors, because formation of these structures is inhibited by the combination of morpholinos and by the VP-*iro7*HD fusion.

In the context of neurogenesis and induction of *ngn1* expression, the interpretation is complicated by the observation that both the activator and repressor forms of *iro7* induce expression of *ngn1*. However, the repressor form is more effective at inducing *ngn1* expression in the ventral ectoderm, while the activator form only induces widespread *ngn1* expression dorsally in the neurectoderm. Furthermore, the repressor form of *iro7* induces *ngn1* expression in a salt-and-pepper pattern, while *iro1* and VP-*iro7*HD induce *ngn1* in a relatively broad domain. One potential explanation for these differences is that Iro genes can act as both activators and repressors and induce *ngn1* expression by different mechanisms in the ventral and dorsal ectoderm. As repressors, Iro genes may indirectly induce *ngn1* expression by inhibiting expression of BMPs and neuralizing the ectoderm. This possibility is supported by the ability of *iro1*, *iro7* and *En-iro7HD* to suppress expression of *gata2*, a BMP target gene. *ngn1* induced in such a manner might more easily be regulated be lateral inhibition and eventually acquire a salt-and-pepper pattern (Ma et al., 1996). However, in the dorsal ectoderm,

which is already neuralized, Iro genes may function as activators to directly induce expression of *ngn1* in a much broader domain. Such a scenario would explain why En-*iro7*HD induces *ngn1* expression a salt-and-pepper pattern in the ventral ectoderm and VP-*iro7*HD induces *ngn1* in a broad domain in the neurectoderm. Wild-type *iro1* may function both as a repressor and activator to induce broad expression of *ngn1* in the ventral ectoderm: as a repressor, it could neuralize the ventral ectoderm; as an activator, it could induce broad expression of *ngn1* in this domain.

Unresolved issues

This study has explored the role of *iro1* and *iro7* in neurogenesis and defined a new role for Iro genes in establishment of an ectodermal compartment following Wnt signaling in vertebrate development. However, many questions remain unanswered. Although ectopic expression of Iro genes can promote *ngn1* expression, endogenous *ngn1* expression is only observed in restricted subdomains of the normal Iro expression domain, suggesting that additional factors regulate *ngn1* expression. Furthermore, when Iro genes induce *ngn1* expression in a broad domain, they inhibit differentiation of neurons, suggesting that Iro genes also induce expression of factors that prevent differentiation [(Bellefroid et al., 1998; Gomez-Skarmeta et al., 1998) and data not shown]. Clarification of the mechanisms that inhibit *ngn1* expression and neuronal differentiation will be necessary to better understand how the Iro genes pattern early neurogenesis.

We have demonstrated that a knockdown of iro1 and iro7 prevents formation of the isthmic organizer at the MHB and it affects patterning in the forebrain and hindbrain. These effects may reflect functions for iro1 and iro7 independent of their role in MHB formation, as previous studies have shown that elimination of the isthmic organizer does not affect forebrain and hindbrain development in a similar manner (Lun and Brand, 1998; Reifers et al., 1998). Further characterization of the changes in forebrain and hindbrain patterning are likely to reveal a relatively early role in the forebrain and a late role in the hindbrain when *iro1* and *iro7* are expressed together in these domains during development. Finally, while loss of *iro1* and *iro7* function prevents formation of the neural crest and the isthmic organizer, ectopic expression of these genes is not sufficient for the formation of these tissues. Identification of factors that work together with Iro genes to determine neural crest fate and MHB identity also remain important directions for future studies.

We thank M. Kacergis and G. Palardy for technical assistance. We are grateful to A. Kawahara, R. Subramanian and I. B. Dawid for critical reading of an earlier version of the manuscript. This work was supported by JSPS research fellowships (M. I.).

REFERENCES

Alexandre, D., Clarke, J. D., Oxtoby, E., Yan, Y. L., Jowett, T. and Holder, N. (1996). Ectopic expression of Hoxa-1 in the zebrafish alters the fate of the mandibular arch neural crest and phenocopies a retinoic acid-induced phenotype. *Development* **122**, 735-746.

Bally-Cuif, L., Cholley, B. and Wassef, M. (1995). Involvement of Wnt-1 in the formation of the mes/metencephalic boundary. *Mech. Dev.* **53**, 23-34.

Bao, Z. Z., Bruneau, B. G., Seidman, J. G., Seidman, C. E. and Cepko, C. L. (1999). Regulation of chamber-specific gene expression in the developing heart by Irx4. *Science* **283**, 1161-1164.

Bellefroid, E. J., Kobbe, A., Gruss, P., Pieler, T., Gurdon, J. B. and Papalopulu, N. (1998). Xiro3 encodes a Xenopus homolog of the Drosophila Iroquois genes and functions in neural specification. *EMBO J.* **17**, 191-203.

Blader, P., Fischer, N., Gradwohl, G., Guillemont, F. and Strahle, U. (1997). The activity of neurogenin1 is controlled by local cues in the zebrafish embryo. *Development* **124**, 4557-4569.

Bosse, A., Stoykova, A., Nieselt-Struwe, K., Chowdhury, K., Copeland, N. G., Jenkins, N. A. and Gruss, P. (2000). Identification of a novel mouse Iroquois homeobox gene, Irx5, and chromosomal localisation of all members of the mouse Iroquois gene family. *Dev. Dyn.* **218**, 160-174.

Bosse, A., Zulch, A., Becker, M. B., Torres, M., Gomez-Skarmeta, J. L., Modolell, J. and Gruss, P. (1997). Identification of the vertebrate Iroquois homeobox gene family with overlapping expression during early development of the nervous system. *Mech. Dev.* **69**, 169-181.

Brand, M., Heisenberg, C. P., Jiang, Y. J., Beuchle, D., Lun, K., Furutani-Seiki, M., Granato, M., Haffter, P., Hammerschmidt, M., Kane, D. A. et al. (1996). Mutations in zebrafish genes affecting the formation of the boundary between midbrain and hindbrain. *Development* **123**, 179-190.

Burglin, T. R. (1997). Analysis of TALE superclass homeobox genes (MEIS, PBC, KNOX, Iroquois, TGIF) reveals a novel domain conserved between plants and animals. *Nucleic Acids Res.* **25**, 4173-4180.

Cavodeassi, F., Diez Del Corral, R., Campuzano, S. and Dominguez, M. (1999). Compartments and organising boundaries in the Drosophila eye: the role of the homeodomain Iroquois proteins. *Development* **126**, 4933-4942.

Cavodeassi, F., Modolell, J. and Campuzano, S. (2000). The Iroquois homeobox genes function as dorsal selectors in the Drosophila head. *Development* **127**, 1921-1929.

Cavodeassi, F., Modolell, J. and Gomez-Skarmeta, J. L. (2001). The iroquois family of genes: from body building to neural patterning. *Development* **128**, 2847-2855.

Chitnis, A. B. (1999). Control of neurogenesis – lessons from frogs, fish and flies. *Curr. Opin. Neurobiol.* **9**, 18-25.

Christoffels, V. M., Keijser, A. G., Houweling, A. C., Clout, D. E. and Moorman, A. F. (2000). Patterning the embryonic heart: identification of five mouse Iroquois homeobox genes in the developing heart. *Dev. Biol.* **224**, 263-274.

Cohen, D. R., Cheng, C. W., Cheng, S. H. and Hui, C. C. (2000). Expression of two novel mouse Iroquois homeobox genes during neurogenesis. *Mech. Dev.* **91**, 317-321.

Conlon, F. L., Sedgwick, S. G., Weston, K. M. and Smith, J. C. (1996). Inhibition of Xbra transcription activation causes defects in mesodermal patterning and reveals autoregulation of Xbra in dorsal mesoderm. *Development* **122**, 2427-2435.

Dambly-Chaudiere, C. and Leyns, L. (1992). The determination of sense organs in Drosophila: a search for interacting genes. *Int. J. Dev. Biol.* **36**, 85-91.

Detrich, H. W. 3rd, Kieran, M. W., Chan, F. Y., Barone, L. M., Yee, K., Rundstadler, J. A., Pratt, S., Ransom, D. and Zon, L. I. (1995). Intraembryonic hematopoietic cell migration during vertebrate development. *Proc. Natl. Acad. Sci. USA* **92**, 10713-10717.

Diez del Corral, R., Aroca, P., Gomez-Skarmeta, J. L., Cavodeassi, F. and Modolell, J. (1999). The Iroquois homeodomain proteins are required to specify body wall identity in Drosophila. *Genes Dev.* **13**, 1754-1761.

Funayama, N., Sato, Y., Matsumoto, K., Ogura, T. and Takahashi, Y. (1999). Coelom formation: binary decision of the lateral plate mesoderm is controlled by the ectoderm. *Development* **126**, 4129-4138.

Glinka, A., Wu, W., Delius, H., Monaghan, A. P., Blumenstock, C. and Niehrs, C. (1998). Dickkopf-1 is a member of a new family of secreted proteins and functions in head induction. *Nature* **391**, 357-362.

Gomez-Skarmeta, J. L., del Corral, R. D., de la Calle-Mustienes, E., Ferre-Marco, D. and Modolell, J. (1996). Araucan and caupolican, two members of the novel iroquois complex, encode homeoproteins that control proneural and vein-forming genes. *Cell* **85**, 95-105.

Gomez-Skarmeta, J. L., Glavic, A., de la Calle-Mustienes, E., Modolell, J. and Mayor, R. (1998). Xiro, a Xenopus homolog of the Drosophila Iroquois complex genes, controls development at the neural plate. *EMBO J.* **17**, 181-190.

Gomez-Skarmeta, J., de La Calle-Mustienes, E. and Modolell, J. (2001). The Wnt-activated Xiro1 gene encodes a repressor that is essential for neural development and downregulates Bmp4. *Development* **128**, 551-560.

Good, P. J. (1995). A conserved family of elav-like genes in vertebrates. *Proc. Natl. Acad. Sci. USA* **92**, 4557-4561.

Goriely, A., Diez del Corral, R. and Storey, K. G. (1999). c-Irx2 expression reveals an early subdivision of the neural plate in the chick embryo. *Mech. Dev.* **87**, 203-206.

Heisenberg, C. P., Houart, C., Take-Uchi, M., Rauch, G. J., Young, N., Coutinho, P., Masai, I., Caneparo, L., Concha, M. L., Geisler, R. et al. (2001). A mutation in the Gsk3-binding domain of zebrafish Masterblind/Axin1 leads to a fate transformation of telencephalon and eyes to diencephalon. *Genes Dev* **15**, 1427-1434.

Hukriede, N. A., Joly, L., Tsang, M., Miles, J., Tellis, P., Epstein, J. A., Barbazuk, W. B., Li, F. N., Paw, B., Postlethwait, J. H. et al. (1999). Radiation hybrid mapping of the zebrafish genome. *Proc. Natl. Acad. Sci. USA* **96**, 9745-9750.

Itoh, M. and Chitnis, A. B. (2001). Expression of proneural and neurogenic genes in the zebrafish lateral line primordium correlates with selection of hair cell fate in neuromasts. *Mech. Dev.* **102**, 263-266.

Jowett, T. (2001). Double in situ hybridization techniques in zebrafish. *Methods* **23**, 345-358.

Kawahara, A., Wilm, T., Solnica-Krezel, L. and Dawid, I. B. (2000). Antagonistic role of vega1 and bozozok/dharma homeobox genes in organizer formation. *Proc. Natl. Acad. Sci. USA* **97**, 12121-12126.

Kessler, D. S. (1997). Siamois is required for formation of Spemann's organizer. *Proc. Natl. Acad. Sci. USA* **94**, 13017-13022.

Kim, C. H., Ueshima, E., Muraoka, O., Tanaka, H., Yeo, S. Y., Huh, T. L. and Miki, N. (1996). Zebrafish elav/HuC homologue as a very early neuronal marker. *Neurosci. Lett.* **216**, 109-112.

Kim, C. H., Bae, Y. K., Yamanaka, Y., Yamashita, S., Shimizu, T., Fujii, R., Park, H. C., Yeo, S. Y., Huh, T. L., Hibi, M. et al. (1997). Overexpression of neurogenin induces ectopic expression of HuC in zebrafish. *Neurosci. Lett.* **239**, 113-116.

Kim, C. H., Oda, T., Itoh, M., Jiang, D., Artinger, K. B., Chandrasekharappa, S. C., Driever, W. and Chitnis, A. B. (2000). Repressor activity of Headless/Tcf3 is essential for vertebrate head formation. *Nature* **407**, 913-916.

Krauss, S., Johansen, T., Korzh, V. and Fjose, A. (1991). Expression of the zebrafish paired box gene pax[zf-b] during early neurogenesis. *Development* **113**, 1193-1206.

Kudoh, T. and Dawid, I. B. (2001). Role of the iroquois3 homeobox gene in organizer formation. *Proc. Natl. Acad. Sci. USA* **98**, 7852-7857.

Kudoh, T., Tsang, M., Hukriede, N. A., Chen, X., Dedekian, M., Clarke, C. J., Kiang, A., Schultz, S., Epstein, J. A., Toyama, R. et al. (2001). A gene expression screen in zebrafish embryogenesis. *Genome Res.* (in press).

Lecaudey, V., Thisse, C., Thisse, B. and Schneider-Maunoury, S. (2001). Sequence and expression pattern of ziro7, a novel, divergent zebrafish iroquois homeobox gene. *Mech. Dev.* **109**, 383-388.

Leyns, L., Gomez-Skarmeta, J. L. and Dambly-Chaudiere, C. (1996). iroquois: a prepattern gene that controls the formation of bristles on the thorax of Drosophila. *Mech. Dev.* **59**, 63-72.

Li, Y., Allende, M. L., Finkelstein, R. and Weinberg, E. S. (1994). Expression of two zebrafish orthodenticle-related genes in the embryonic brain. *Mech. Dev.* **48**, 229-244.

Lun, K. and Brand, M. (1998). A series of no isthmus (noi) alleles of the zebrafish pax2.1 gene reveals multiple signaling events in development of the midbrain-hindbrain boundary. *Development* **125**, 3049-3062.

Ma, Q., Kintner, C. and Anderson, D. J. (1996). Identification of neurogenin, a vertebrate neuronal determination gene. *Cell* **87**, 43-52.

Marchant, L., Linker, C., Ruiz, P., Guerrero, N. and Mayor, R. (1998). The inductive properties of mesoderm suggest that the neural crest cells are specified by a BMP gradient. *Dev. Biol.* **198**, 319-329.

McClintock, J. M., Carlson, R., Mann, D. M. and Prince, V. E. (2001). Consequences of Hox gene duplication in the vertebrates: an investigation of the zebrafish Hox paralogue group 1 genes. *Development* **128**, 2471-2484.

Mori, H., Miyazaki, Y., Morita, T., Nitta, H. and Mishina, M. (1994). Different spatio-temporal expressions of three otx homeoprotein transcripts during zebrafish embryogenesis. *Mol. Brain Res.* **27**, 221-231.

Nguyen, M., Park, S., Marques, G. and Arora, K. (1998). Interpretation of a BMP activity gradient in Drosophila embryos depends on synergistic signaling by two type I receptors, SAX and TKV. *Cell* **95**, 495-506.

Odenthal, J. and Nusslein-Volhard, C. (1998). fork head domain genes in zebrafish. *Dev. Genes Evol.* **208**, 245-258.

Ogura, K., Matsumoto, K., Kuroiwa, A., Isobe, T., Otoguro, T., Jurecic, V., Baldini, A., Matsuda, Y. and Ogura, T. (2001). Cloning and chromosome mapping of human and chicken Iroquois (IRX) genes. *Cytogenet Cell Genet.* **92**, 320-325.

Oxtoby, E. and Jowett, T. (1993). Cloning of the zebrafish krox-20 gene (krx-20) and its expression during hindbrain development. *Nucleic Acids Res.* **21**, 1087-1095.

Patapoutian, A. and Reichardt, L. F. (2000). Roles of Wnt proteins in neural development and maintenance. *Curr. Opin. Neurobiol.* **10**, 392-399.

Peters, T., Dildrop, R., Ausmeier, K. and Ruther, U. (2000). Organization of mouse Iroquois homeobox genes in two clusters suggests a conserved regulation and function in vertebrate development. *Genome Res.* **10**, 1453-1462.

Reifers, F., Bohli, H., Walsh, E. C., Crossley, P. H., Stainier, D. Y. and Brand, M. (1998). Fgf8 is mutated in zebrafish acerebellar (ace) mutants and is required for maintenance of midbrain-hindbrain boundary development and somitogenesis. *Development* **125**, 2381-2395.

Rhinn, M. and Brand, M. (2001). The midbrain–hindbrain boundary organizer. *Curr. Opin. Neurobiol.* **11**, 34-42.

Schwarz, M., Alvarez-Bolado, G., Urbanek, P., Busslinger, M. and Gruss, P. (1997). Conserved biological function between Pax-2 and Pax-5 in midbrain and cerebellum development: evidence from targeted mutations. *Proc. Natl. Acad. Sci. USA* **94**, 14518-14523.

Tan, J. T., Korzh, V. and Gong, Z. (1999). Expression of a zebrafish iroquois homeobox gene, Ziro3, in the midline axial structures and central nervous system. *Mech. Dev.* **87**, 165-168.

Wang, X., Emelyanov, A., Sleptsova-Friedrich, I., Korzh, V. and Gong, Z. (2001). Expression of two novel zebrafish iroquois homologues (ziro1 and ziro5) during early development of axial structures and central nervous system. *Mech. Dev.* **105**, 191-195.

Wurst, W. and Bally-Cuif, L. (2001). Neural plate patterning: upstream and downstream of the isthmic organizer. *Nat. Rev. Neurosci.* **2**, 99-108.